

KECK MEASUREMENT OF THE XTE J2123–058 RADIAL VELOCITY CURVE

JOHN A. TOMSICK AND WILLIAM A. HEINDL

Center for Astrophysics and Space Sciences, University of California, San Diego, MS 0424, La Jolla, CA 92093

DEEPTO CHAKRABARTY

Department of Physics and Center for Space Research, Massachusetts Institute of Technology, Cambridge, MA 02139

JULES P. HALPERN

Columbia Astrophysics Laboratory, Columbia University, 550 West 120th Street, New York, NY 10027

PHILIP KAARET

Harvard-Smithsonian Center for Astrophysics, 60 Garden Street, Cambridge, MA 02138

Submitted to ApJ Letters

ABSTRACT

We measured the radial velocity curve of the companion of the neutron star X-ray transient XTE J2123–058. Its semi-amplitude (K_2) of $298.5 \pm 6.9 \text{ km s}^{-1}$ is the highest value that has been measured for any neutron star LMXB. The high value for K_2 is, in part, due to the high binary inclination of the system but may also indicate a high neutron star mass. The mass function (f_2) of $0.684 \pm 0.047 M_\odot$, along with our constraints on the companion's spectral type (K5V–K9V) and previous constraints on the inclination, gives a likely range of neutron star masses from 1.2 to $1.8 M_\odot$. We also derive a source distance of $8.5 \pm 2.5 \text{ kpc}$, indicating that XTE J2123–058 is unusually far, $5.0 \pm 1.5 \text{ kpc}$, from the Galactic plane. Our measurement of the systemic velocity is $-94.5 \pm 5.5 \text{ km s}^{-1}$, confirming that this is a high velocity object and supporting the hypothesis that it was ejected from the Galactic plane at high velocity.

Subject headings: accretion, accretion disks — X-ray transients: general — stars: individual (XTE J2123–058)
— stars: neutron stars — X-rays: stars

1. INTRODUCTION

The X-ray transient XTE J2123–058 is a neutron star low mass X-ray binary (LMXB) that was discovered in 1998 (Levine, Swank & Smith, 1998). We optically identified the transient (Tomsick et al., 1998a) and determined the ~ 6 hour binary orbital period (Tomsick et al., 1998b). Type I X-ray bursts indicate that the system contains a neutron star, and the relatively short orbital period indicates that the companion is a late-type star on or close to the main sequence. A pair of high frequency quasi-periodic oscillations was detected, which may indicate a rapidly rotating neutron star (Homan et al., 1999; Tomsick et al., 1999). XTE J2123–058 distinguishes itself from other LMXBs by having high Galactic latitude ($b = -36^\circ$) and also a high binary inclination ($i \sim 73^\circ$, Zurita et al. 2000). Both of these properties are advantageous for determining the mass of the neutron star from optical observations in quiescence, which is the primary goal of this work.

Neutron star mass measurements are important for fundamental physics and for understanding the evolution of neutron star systems. Although precise neutron star mass measurements have been made for several millisecond radio pulsars (MSPs), such measurements are lacking for LMXBs. Since it is theoretically possible to spin-up neutron stars in LMXBs to millisecond periods via accretion, a link between LMXBs and MSPs has long been suspected (Alpar et al., 1982). If this picture is correct, we expect a large fraction of the neutron stars in LMXBs to be spinning at millisecond periods, and for the spun-up neutron stars in LMXBs and in MSPs to be more massive by 0.1 to $0.5 M_\odot$ (Bhattacharya 1995) than neutron stars that have not been spun-up. Surprisingly, an analysis of binary MSPs found no definite evidence for neutron stars with masses above the Chandrasekhar mass limit of $1.4 M_\odot$ (Thorsett & Chakrabarty,

1999). This makes it critical to measure the masses of neutron stars in LMXBs to determine if they are above $1.4 M_\odot$. Mass measurements may also place important constraints on the neutron star equation of state.

2. OBSERVATIONS AND DATA REDUCTION

In 2000 August, we performed spectroscopy of XTE J2123–058 with the Echelle Spectrograph and Imager (ESI, Sheinis et al. 2000) at Keck Observatory. As shown in Table 1, we took eight exposures over two nights covering one 6 hour binary orbit. The cross-dispersed spectra were taken in Echelle mode with ten spectral orders falling on a 2048-by-4096 pixel CCD. We performed on-chip rebinning to 2048-by-2048 pixels to decrease read noise. Although this instrument is sensitive from 3900–11000 Å, we only used the data in the 4700–6820 Å band for this work. In this band, the dispersion varies from 0.36 to 0.52 Å per pixel (after rebinning). This is sufficient to oversample the resolution of the spectrograph as we used a $1''$ slit, providing a spectral resolution of 1.0 to 1.5 Å FWHM .

We obtained R and V-band photometry of XTE J2123–058 at MDM Observatory 10 days before the Keck observations, and found values for R and V consistent with the quiescent magnitudes reported in Tomsick et al. (1999). We measured $V = 22.68 \pm 0.11$ (corrected for atmospheric extinction but not reddening), and we use this value below to determine the source distance. Due to the faintness of the source, relatively long exposure times between 2340 and 2700 seconds were necessary for our spectroscopic observations. However, even these long exposures are a relatively small fraction of the orbital period. We obtained M, K and G dwarf comparison star spectra for the cross-correlations described below.

We extracted the spectra using the software package “ma-

TABLE 1
XTE J2123–058 KECK OBSERVATIONS

Exposure	MJD ^a (days)	Exposure Time (seconds)	FWHM Seeing (arcseconds)
1	51759.39442	2700	0.87
2	51759.42822	2510	0.91
3	51759.45771	2510	1.23
4	51759.48768	2510	0.79
5	51759.51748	2400	0.85
6	51759.54536	2340	0.98
7	51759.57288	2340	0.86
8	51760.35770	2400	0.67

^aModified Julian Date (JD–2400000.5) at the midpoint of the exposure.

kee” which was originally developed for the HIRES instrument at Keck, but has been adapted to extract ESI spectra. Using makee, we defined source and background regions and produced an optimally extracted spectrum for each of the ten spectral orders. We obtained CuAr line lamp exposures at the beginning and end of each night to determine the wavelength solution, and we checked this solution for each exposure using OI and NaI night sky lines. Averaging over all exposures and night sky lines, the difference between measured and actual wavelengths is 0.018Å. The calibration is also stable from exposure-to-exposure with a standard deviation of 0.027Å or less for all night sky lines, indicating that time variability of the wavelength solution introduces an error of less than 1.5 km s^{–1} into our radial velocity measurements. The data reduction procedure includes heliocentric velocity and atmospheric extinction corrections. We used IRAF routines to flux calibrate the spectra and obtained exposures of the spectrophotometric standard Hiltner 102 (Stone, 1977) on both nights for this purpose. To produce the final spectra, we combined the spectral orders after flux calibration. In the process of combining the orders, we rebinned the spectra to a log-linear wavelength scale with 22.8 km s^{–1} pixels. Finally, we dereddened the XTE J2123–058 spectra using $A_V = 0.37$ magnitudes (Hynes et al., 2001).

The quality of the XTE J2123–058 spectra varies significantly between exposures as indicated by the signal-to-noise ratios (SNR) given in Table 2. The mean SNR per pixel in the 5650–5850Å band is 1.66 in the worst case and 6.63 in the best case. One reason for this is that the source shows large orbital flux variations as can be seen from the fluxes given in Table 2. The flux variations show two peaks per orbit (exposures 5 and 8), which is expected if the variability is caused by ellipsoidal modulations. XTE J2123–058 light curves from optical photometry show that ellipsoidal modulations are indeed present (Zurita et al., 2000). In addition to changes in flux, the SNR variations are caused by variable seeing as shown in Table 1. The FWHM seeing for the exposure taken on the second night is 0''.67 compared to an average of 0''.93 for the exposures on the first night. It should be noted that the Table 2 fluxes are not corrected for seeing.

3. RESULTS

3.1. Cross-Correlations

Our analysis of the spectra focuses on the region from 4700Å to 6820Å since the SNR becomes very poor below 4700Å and night sky lines dominate the spectrum above 6820Å. In this

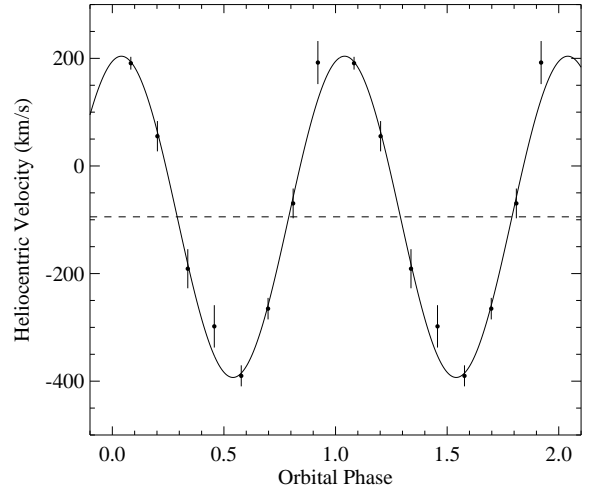


FIG. 1.— Radial velocity curve fitted using a sinusoid with the parameters given in Table 3 and folded on the orbital period. Heliocentric velocities are shown (with errors increased by 60% over the values given in Table 2), and the dashed line marks the systemic velocity. The data are plotted twice for clarity.

band, the spectra show features from the accretion disk ($H\alpha$ and $H\beta$ emission lines) and from the companion star. An examination of the spectra clearly shows the presence of a wide depression centered between 5100 and 5200Å. This is the signature of a K-type star and is due to the MgH feature at 5180Å, the TiO band at 4954–5200Å and a continuum discontinuity associated with the MgI triplet at 5168–5185Å (McClintock & Remillard 1990 and references therein). An absorption feature is seen near 5900Å due to the NaI doublet at 5891–5898Å. The strength of this feature indicates a late-K spectral type for the companion.

We used the IRAF routine “fxcor” (Tonry & Davis, 1979; Filippenko, Matheson & Ho, 1995) to cross-correlate the XTE J2123–058 spectra with the comparison stars. After masking night sky lines at 5205, 5579, 5891, 5898 and 6302Å and the $H\alpha$ and $H\beta$ emission lines from the source, we used the wavelength bands 4890–5190, 5210–5560, 5630–5860, 5985–6135 and 6640–6820Å for the cross-correlations. We also applied a bandpass filter from 30 to 800 cycles per spectrum in order to remove contributions due to spurious variations in the continuum and high frequency noise. We calculated cross-correlations for G0V, G5V, G9V, K0V, K2V, K4V, K7V, M0V and M1V with the exposure 8 spectrum. Highly significant peaks with Tonry & Davis (1979) R-values between 8.9 and 16.3 at roughly the same velocity occur, with the M-type and GOV stars giving the weakest correlations and the K7V star (HD 88230) giving the strongest correlation. For this reason and because of the strong NaI line, we used the K7V star for the radial velocity study.

We obtained unique and significant cross-correlation peaks at reasonable velocities (–1000 to 1000 km s^{–1}) for all eight exposures. The measured heliocentric velocities range from –390 km s^{–1} to 192 km s^{–1} and are given in Table 2. The R-values vary significantly from 3.3 to 16.3 due to SNR differences. Figure 1 shows the radial velocity curve. First, we performed a least-squares fit to the data with a function consisting

TABLE 2
FLUXES, SIGNAL-TO-NOISE RATIOS AND CROSS-CORRELATION
RESULTS

Exposure	Flux ^a	SNR ^b	R ^c	Measured RV ^d	Fitted RV ^e
1	1.24	1.66	3.26	55.3 ± 17.6	63.2
2	1.72	2.66	4.29	-191.0 ± 22.7	-182.4
3	1.53	2.15	4.54	-298.1 ± 24.6	-352.8
4	2.90	4.40	8.88	-390.1 ± 12.2	-385.0
5	3.06	4.18	8.82	-265.2 ± 12.5	-259.0
6	2.48	2.87	5.14	-69.6 ± 17.3	-58.1
7	2.32	2.41	3.35	192.2 ± 25.0	123.6
8	5.53	6.63	16.32	191.0 ± 7.4	193.5

^aMean flux in the 5650 to 5850 Å band in units of 10^{-18} erg cm⁻² s⁻¹ Å⁻¹.

^bMean signal-to-noise ratio per pixel in the 5650 to 5850 Å band.

^cTonry & Davis (1979) R-value

^dMeasured heliocentric radial velocity in km s⁻¹ with Tonry & Davis (1979) errors.

^eHeliocentric radial velocity in km s⁻¹ based on a sinusoidal fit to the data.

of a constant plus a sinusoid with four free parameters: the systemic velocity (γ), the epoch of inferior conjunction (T_0), the radial velocity semi-amplitude (K_2) and the orbital period (P_{orb}). This does not provide a formally acceptable fit ($\chi^2/\nu = 12/4$) so we increased the errors on the individual velocity measurements by 60% to give a reduced χ^2 of 1.0. The fit gives a large range of possible values for P_{orb} with a 90% confidence error region from 21125 to 22575 seconds. This range contains the photometric orbital period of 21445.5 ± 2.3 seconds measured previously (Tomsick et al., 1999; Illovaisky & Chevalier, 1998; Zurita et al., 2000), and we refitted the radial velocity curve after fixing P_{orb} to this value. We expect that the photometric and spectroscopic orbital periods are the same since the photometric value is based on partial eclipses seen in the optical light curve during outburst (Tomsick et al., 1999; Zurita et al., 2000).

Table 3 shows the fit parameters with P_{orb} fixed, and this fit is shown in Figure 1. Its semi-amplitude (K_2) of 298.5 ± 6.9 km s⁻¹ is the highest value that has been measured for any neutron star LMXB. The value of -94.5 ± 5.5 km s⁻¹ for γ is consistent with the tentative value of -90 km s⁻¹ derived from emission lines (Hynes et al., 2001). We note that previous measurements of the photometric epoch are too uncertain to make a meaningful comparison to our spectroscopic epoch.

3.2. Average Spectrum and Source Distance

We produced an average, Doppler corrected spectrum using the eight XTE J2123–058 exposures. We first removed pixels that were contaminated by night sky lines. Next, we multiplied each spectrum by a constant based on the fluxes given in Table 2 to establish a common normalization. This is important because the wavelength bins near night sky lines do not have contributions from all eight exposures. We then Doppler corrected the spectra using the fitted radial velocity values given in Table 2. Finally, the spectra were interpolated to a common set of wavelength bins, and a weighted average was calculated for each wavelength bin.

The average spectrum is shown in Figure 2 along with the spectrum of HD 88230. Gaussian fits to the XTE J2123–058 emission lines give equivalent widths (EW) of 15.8 and 17.6 Å and FWHM widths of 1443 ± 64 and 1729 ± 133 km s⁻¹ for H α and H β , respectively. The FWHM widths are signif-

icantly less for the individual exposures. The continuum features near 5000–5300 Å are similar to HD 88230, and narrow MgI absorption lines are seen in both spectra near the break in the continuum. Matching absorption lines are also present in several other parts of the spectrum, including the NaI doublet at 5891–5898 Å.

We fitted the region of the spectrum near the NaI doublet with a constant plus two inverted Gaussians for the XTE J2123–058 average spectrum and also for the comparison stars in order to determine the total EW of the NaI doublet. For XTE J2123–058, we measure an EW of 3.1 ± 0.6 Å (after correcting for interstellar absorption using results from Hynes et al. 2001). For the K0V, K2V, K4V, K7V and M1V comparison stars, we measure EW of 1.1, 2.5, 3.6, 6.9 and 7.2 Å, respectively. Since the H α and H β emission lines indicate a significant disk contribution, these EW values indicate that the spectral type of the companion is later than K4V. However, based on the strengths of the cross-correlation peaks described above, the companion is a K rather than an M-type star. The range of possible spectral types is K5V–K9V.

We determined the source distance using the method described by McClintock et al. (2001). We assume a spectral type of K7V in the calculation and discuss possible associated uncertainties below. The strength of the NaI doublet indicates that the fraction of the light coming from the companion at 5900 Å is $45\% \pm 8\%$. This, along with the MDM measurement ($V = 22.68$), gives an effective V-magnitude for the companion of 23.56. We calculated the absolute V-magnitude (M_V) of the companion using the expression given in Popper (1980), which depends on the spectral type and the radius of the companion. Since the companion fills its Roche lobe, its average density depends only on the orbital period (Faulkner, Flannery & Warner, 1972). From the density and assuming that the companion mass is $0.4 M_\odot$, which is likely correct to within a factor of two (Barret, McClintock & Grindlay, 1996), we estimate a radius of $0.56 R_\odot$ for the companion. This radius and the K7V spectral type gives $M_V = 8.42$. After accounting for extinction, we obtained a source distance of 9.0 kpc. Recalculating with different spectral types indicates that the error associated with the K5V–K9V range is ± 1 kpc. Also, the factor of two uncertainty in the companion’s mass translates to a 25% uncertainty in the distance (McClintock et al., 2001). Finally, there is a systematic error due to orbital variations in the V-magnitude. The MDM observations were made close to photometric minimum so that the average V-magnitude is somewhat less than 22.68. Based on the quiescent light curve shown in Zurita et al.

TABLE 3
SPECTROSCOPIC PARAMETERS

Parameter	Result ^a
Epoch ^b	$T_0 = \text{HJD } 2451760.0462 \pm 0.0013$ days
Systemic Velocity	$\gamma = -94.5 \pm 5.5$ km s ⁻¹
Velocity Semi-Amplitude	$K_2 = 298.5 \pm 6.9$ km s ⁻¹
Orbital Period ^c	$P_{orb} = 21445.5$ seconds

^a68% confidence errors are given.

^bHeliocentric Julian Date of the epoch of inferior conjunction.

^cOrbital period determined from photometry (Tomsick et al., 1999; Illovaisky & Chevalier, 1998; Zurita et al., 2000).

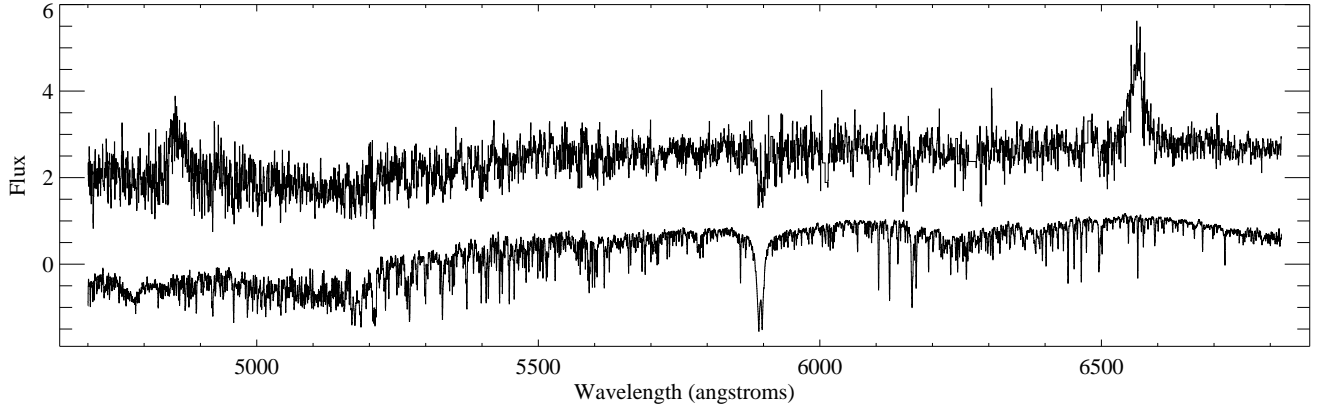


FIG. 2.— The top spectrum shows the average, Doppler corrected spectrum for XTE J2123–058 in units of $10^{-18} \text{ erg cm}^{-2} \text{ s}^{-1} \text{ Å}^{-1}$. $\text{H}\alpha$ and $\text{H}\beta$ emission lines are present at 6564 Å and 4863 Å . The spectrum for the K7V comparison star (HD 88230) is shown below and the units are arbitrary. Several matching features between XTE J2123–058 and HD 88230 are present including the continuum break near 5200 Å and the NaI doublet at $5891\text{--}5898 \text{ Å}$.

(2000), we estimate that the average V-magnitude is close to 22.55, which decreases the distance by 0.5 kpc. We conclude that the distance is $8.5 \pm 2.5 \text{ kpc}$, indicating that XTE J2123–058 is $5.0 \pm 1.5 \text{ kpc}$ from the Galactic plane.

4. DISCUSSION AND CONCLUSIONS

From K_2 and P_{orb} , we derive a mass function of $f_2 = 0.684 \pm 0.047 M_\odot$, representing a lower limit on the neutron star mass (M_1). The binary inclination (i) and the mass ratio ($q = M_1/M_2$) are also necessary to obtain a precise measurement of M_1 . For XTE J2123–058, $i = 73^\circ \pm 4^\circ$ was determined via modeling of the outburst optical light curves (Zurita et al., 2000). Figure 3 shows M_1 vs. M_2 using the measured values of f_2 and i . From our constraint on the spectral type of the companion (K5V–K9V), it is very likely that M_2 lies between 0.4 and $0.7 M_\odot$. For this range of companion masses, the range of neutron star masses is $1.2\text{--}1.8 M_\odot$. Accurate determination of q , which may be possible via measurements of the rotational broadening of the secondary or light curve modeling, is critical to improve the mass constraint. Finding that the neutron star mass is near the upper end of the $1.2\text{--}1.8 M_\odot$ mass range would have important implications for neutron star equations of state, and, in general, determining the mass has important implications for the evolu-

tion of neutron star systems.

In addition to our measurement of f_2 and the constraints on the neutron star mass, our results also confirm that XTE J2123–058 is unusually far from the Galactic plane. The systemic radial velocity of -94.5 km s^{-1} indicates a large peculiar velocity since differential Galactic rotation gives a positive radial velocity ($l = 46.5^\circ$ for XTE J2123–058). Homan et al. (1999) indicate that space velocities of $150\text{--}400 \text{ km s}^{-1}$ are necessary for a system to reach a distance from the Galactic plane comparable to that observed for XTE J2123–058 if it originates in the plane. Although a direct comparison would require a proper motion measurement, the high radial velocity is evidence in favor of this scenario.

We especially wish to thank John O’Meara for his help with observations at Keck and also for useful discussions concerning data reduction. We also thank Tom Barlow for assistance in using his makee software. We acknowledge Judy Cohen for obtaining a standard star exposure for us during her Keck run, and Bob Goodrich for his help with ESI. We thank Gary Puniwai and Charles Sorenson for assistance with the telescope.

References

- Alpar, M. A., Cheng, A. F., Ruderman, M. A., & Shaham, J., 1982, *Nature*, 300, 728
- Barret, D., McClintock, J. E., & Grindlay, J. E., 1996, *ApJ*, 473, 963
- Bhattacharya, D., 1995, *X-ray Binaries*, (Cambridge: Cambridge U. Press)
- Faulkner, J., Flannery, B. P., & Warner, B., 1972, *ApJ*, 175, L79
- Filippenko, A. V., Matheson, T., & Ho, L. C., 1995, *ApJ*, 455, 614
- Homan, J., Méndez, M., Wijnands, R., van der Klis, M., & van Paradijs, J., 1999, *ApJ*, 513, 119
- Hynes, R., et al., 2001, *MNRAS*, accepted, astro-ph/0101104
- Ilovaisky, S. A., & Chevalier, C., 1998, *IAU Circular*, 6975
- Levine, A., Swank, J., & Smith, E., 1998, *IAU Circular*, 6955
- McClintock, J., et al., 2001, *ApJ*, astro-ph/0101421
- McClintock, J. E., & Remillard, R. A., 1990, *ApJ*, 350, 386
- Popper, D. M., 1980, *ARA&A*, 18, 115
- Sheinis, A., Miller, J., Bolte, M., & Sutin, B., 2000, *SPIE*, 4008
- Stone, R. P. S., 1977, *ApJ*, 218, 767
- Thorsett, S. E., & Chakrabarty, D., 1999, *ApJ*, 512, 288
- Tomsick, J. A., Halpern, J. P., Kemp, J., & Kaaret, P., 1999, *ApJ*, 521, 341
- Tomsick, J. A., Halpern, J. P., Leighly, K. M., & Perlman, E., 1998a, *IAU Circular*, 6957
- Tomsick, J. A., Kemp, J., Halpern, J. P., & Hurley-Keller, D., 1998b, *IAU Circular*, 6972
- Tonry, J., & Davis, M., 1979, *AJ*, 84, 1511
- Zurita, C., et al., 2000, *MNRAS*, 316, 137

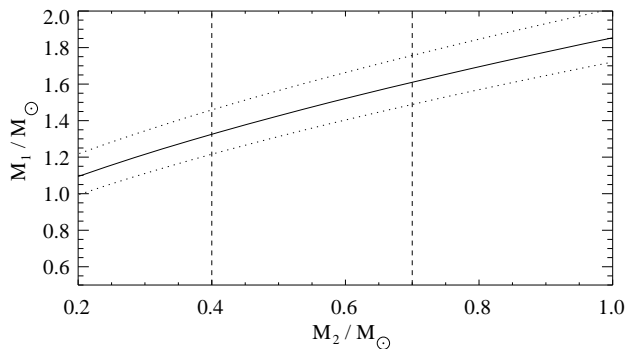


FIG. 3.— The neutron star mass (M_1) vs. the companion mass (M_2). The solid line comes from the values of f_2 and i given in the text, and the dotted lines are based on the extremes of the error regions for these parameters. The vertical dashed lines mark the likely range for M_2 .